Supplementary Material

1 SUPPLEMENTARY METHODS

1.1 SIR model

Mortality rates, and rates of severe illness that do not result in death but require long-term (≥14 days) hospitalization and are likely to have post-infection impacts on health, both reduce $E_i(t)$, and are combined additively to yield ϕ_i (text Equation 4). The rates are obtained from a SIR (Susceptible, Infected, Removed) epidemiological model Kermack and McKendrick (1927). The SIR model is the most basic compartmental epidemiological model that provides time series estimates of the number of people in a population who have completed the infectious phase either because of survival or death. Here, survival may refer to a range of conditions, including long-term disablement. The SIR model consists of three coupled ordinary differential equations,

$$\frac{dS}{dt} = -\frac{\beta IS}{N} \tag{S1}$$

$$\frac{dI}{dt} = \frac{\beta IS}{N} - \gamma I \tag{S2}$$

$$\frac{dR}{dt} = \gamma I \tag{S3}$$

where S is the number of susceptible individuals in the population, I is the number infected, and R the number removed because of death or recovery (not to be confused with the R that signifies growth rate of the epidemic, that is, R_0 and R_{eff}); N is the total population size. β is the average number of contacts of an infected individual per unit time, and is estimated as the quotient of R_0 and the average duration of the disease, set here at 14 days during the first COVID-19 wave; thus $\beta = R_0/14$. In order to estimate β and γ, we relied on published estimates of R_0, the expected number of secondary infected cases expected from an initial infected individual (see Supplementary Material Section 1.1.1). β, the contact rate between susceptible and infected individuals was then estimated here as the average number of contacts of an infected individual per unit time given the average duration of the disease, set here at 14 days during the first COVID-19 wave; thus $\beta = R_0/14$. γ is the rate at which infectious individuals are removed from the population because of death or recovery, and was estimated as the inverse of the average time for which infected individuals remain infectious, 10 days in the case of COVID-19 (US Centers for Disease Control and Prevention).

Age classes used for tracking by the US CDC are not commensurate with those used by the USBLS for worker ages, so United States Census Bureau (USCB) data were aggregated in the following manner to obtain rates for the coupled SIR-CASES model. The model compartment for ages 5-17 years used USCB data for workers 17 years and younger; 18-49 years aggregated data from USCB category 18-44 years plus half the number of workers recorded for the 45-54 years category; the 50-64 years compartment aggregated data of half the number recorded by the USCB for the 45-54 years category plus the 55-64 years category; and the 65 years plus compartment was equal to the 65 years and over USCB category. Data were specific to each SES, and were used to generate age fractions per compartment per industrial sector for each SES.

1.1.1 R_0

Each SES examined in the study had an estimated R_0 on March 1, 2020, based on ensemble estimates from the California Department of Public Health's California COVID Assessment Tool (CalCAT) Tool (2020), derived from COVID Act Now Henderson et al. (2020), COVID19Projections.com Gu (2020), the University of California Los Angeles Zou et al. (2020), LEMMA Schwab (2020), Johns Hopkins University Lemaitre et al. (2020), Stanford University Goldhaber-Fiebert et al. (2020), University of California San Francisco Worden et al. (2020), and Harvard University Lin (2020) models. Ensemble estimates were either available for each SES, or were taken from estimates for the demographically largest county in an SES (Supplementary Table S1). The results presented here are based on the California Department of Public Health's ensemble estimates of R_0, but the results of applying each of the eight component models separately are presented in Supplementary Fig. S1.

The growth rate of a disease is not constant during a typical epidemic, and can respond to numerous factors, such as changes of virulence, and societal measures, including improved treatments, social distancing and quarantines. Here we assumed R_0 to be constant during the first year of a simulation because the business-as-usual scenario means that no mitigation measures are taken to reduce it. The SIR parameters were therefore estimated from a single initial value of R0 as explained above. We also assume a constant contagiousness of the SARS-CoV-2 virus during that year, although newer more infectious strains have swept through populations since the start of the pandemic, and continue to do so Plante et al. (2020); Hou et al. (2020); Volz et al. (2020); Mishra et al. (2021).

REFERENCES

[Dataset] Goldhaber-Fiebert, J., Alarid-Escudero, F., and Andrews, J. (2020). Stanford-CIDE Coronavirus Simulation Model (SC-COSMO) –Technical Description Document, Version 1.0. https://tinyurl.com/ya4rdhys

[Dataset] Gu, Y. (2020). Model details. https://tinyurl.com/y83gm22f

[Dataset] Henderson, M., Carlson, E., Kofman, I., Kreiss-Tomkins, J., and Blech, A. (2020). Covid Act Now Assumptions And References. https://tinyurl.com/yb8kadkz

Hou, Y. J., Chiba, S., Halfmann, P., Ehre, C., Kuroda, M., Dinnon, K. H., et al. (2020). SARS-CoV-2 D614G variant exhibits efficient replication ex vivo and transmission in vivo. Science 370, 1464–1468

Kermack, W. O. and McKendrick, A. G. (1927). A contribution to the mathematical theory of epidemics. Proceedings of the Royal Society of London. Series A 115, 700–721

Lemaitre, J. C., Grantz, K. H., Kaminsky, J., Meredith, H. R., Truelove, S. A., Lauer, S. A., et al. (2020). A scenario modeling pipeline for COVID-19 emergency planning. medRxiv doi:10.1101/2020.06.11.20127894

[Dataset] Lin, X. (2020). Visualizing COVID-19's Effective Reproduction Number (Rt). http://metrics.covid19-analysis.org/

Mishra, S., Mindermann, S., Sharma, M., Whittaker, C., Mellan, T. A., Wilton, T., et al. (2021). Changing composition of SARS-CoV-2 lineages and rise of Delta variant in England. EClinicalMedicine 39, 101064

Plante, J. A., Liu, Y., Liu, J., Xia, H., Johnson, B. A., Lokugamage, K. G., et al. (2020). Spike mutation D614G alters SARS-CoV-2 fitness. Nature , 1–9doi:10.1038/s41586-020-2895-3

[Dataset] Schwab, J. (2020). LEMMA (Local Epidemic Modeling for Management & Action). https://tinyurl.com/yag8o9wy

[Dataset] Tool, C. C. A. (2020). Modeling COVID-19 to Inform State and Local Response. https://tinyurl.com/y2yzakgy

Volz, E., Hill, V., McCrone, J. T., Price, A., Jorgensen, D., O'Toole, Á., et al. (2020). Evaluating the effects of SARS-CoV-2 Spike mutation D614G on transmissibility and pathogenicity. Cell doi:10.1016/j.cell.2020.11.020

Worden, L., Wannier, R., Neus, M., Kwan, J. C., Ge, A. Y., Richardson, E. T., et al. (2020). Estimation of COVID-19 transmission rates in California and the U.S. with reporting delays. medRxiv doi:10.1101/2020.05.14.20101162

Zou, D., Wang, L., Xu, P., Chen, J., Zhang, W., and Gu, Q. (2020). Epidemic model guided machine learning for COVID-19 forecasts in the United States. medRxiv doi:10.1101/2020.05.24.20111989

Table S1. SES R0 values on March 1, 2020. Values were estimated for multi-county SESs based on the largest county in the aggregate, indicated in the "County" column. In the case of the San Jose-Sunnyvale-Santa Clara SES, there is a large difference between Santa Clara and San Benito counties, 1.55 and 2.4 respectively. Those values were therefore combined as an average weighted by the population sizes of each county.

SES	County	R_0
Oakland-Berkeley-Livermore	Alameda	1.89
San Francisco-San Mateo-Redwood City	San Francisco	2.35
San Jose-Sunnyvale-Santa Clara	Santa Clara San Benito	1.59
Stockton-Lodi	San Joaquin	2.63
Fresno	Fresno	2.57
Oxnard-Thousand Oaks-Ventura	Ventura	2.48
Los Angeles-Glendale-Long Beach	Los Angeles	2.34
Anaheim-Santa Ana-Irvine	Orange	2.32
Riverside-San Bernardino-Ontario	Riverside	2.09
San Diego-Carlsbad	San Diego	1.95

Table S2. Nonlinear regression coefficients of unemployment on day 151 on R0 . The function is of the form b0/[1 + exp[b1 (R0 + b2)]]. $r^2 > 0.999$ and $p < 0.0001$ for all socio-economic systems (SESs).

SES	b_0	b_1	b_2
Oakland-Berkeley-Livermore	0.052	-5.535	-2.371
San Francisco-San Mateo-Redwood City	0.087	-5.649	-2.357
San Jose-Sunnyvale-Santa Clara	0.090	-5.655	-2.356
Stockton-Lodi	0.112	-5.770	-2.341
Fresno	0.137	-5.869	-2.329
Oxnard-Thousand Oaks-Ventura	0.082	-5.646	-2.357
Los Angeles-Long Beach-Glendale	0.051	-5.537	-2.370
Anaheim-Santa Ana-Irvine	0.059	-5.561	-2.368
Riverside-San Bernardino-Ontario	0.044	-5.526	-2.372
San Diego-Carlsbad	0.073	-5.671	-2.361

Table S3. Multivariate regression of cascade logistic parameters on PC1 SES scores. r – maximum growth rate of unemployment with increasing R_0 ("tipping point"); K – asymptotic level of unemployment.

Equation	Obs	Paramaters	RMSE	R^2	F	p
r	10	2	0.091	0.311	3.614	0.094
K	10	2	0.018	0.668	16.122	0.004
	Coeff.	Std. err.	t	$p{>}\|t\|$	95% CI	
r						
pcb1	-0.017	0.009	-1.90	0.094	-0.037	0.003
cons	5.748	0.029	199.56	0.000	5.682	5.814
K						
pcb1	-0.007	0.002	-4.02	0.004	-0.011	-0.003
cons	0.068	0.0057	11.90	0.000	0.055	0.082

2 SUPPLEMENTARY TABLES AND FIGURES

2.1 Figures

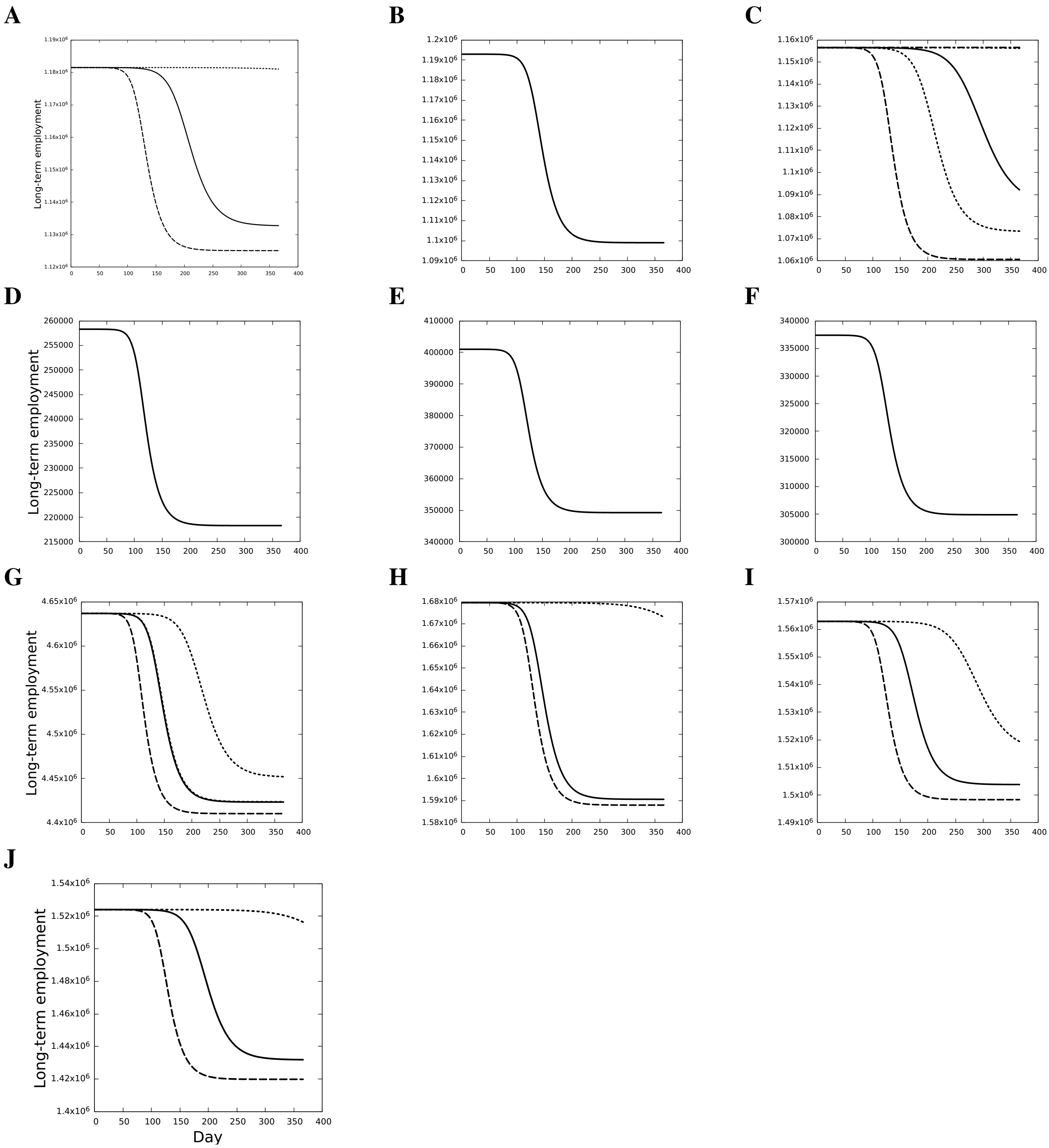

Figure S1. CASES cascade model simulation output for individual model estimate of R_0 on March 1, 2020. Solid black line represents ensemble estimates of individual models. Additional lines correspond to the following individual models: small dots-COVID-19 projections; long dash-Johns Hopkins University; dash dot-University of California San Francisco; large dots-Stanford University. (*A*)-(*J*) respectively: Oakland-Berkeley-Livermore, San Francisco-San Mateo-Redwood City, San Jose-Sunnyvale-Santa Clara, Stockton-Lodi, Fresno, Oxnard-Thousand Oaks-Ventura, Los Angeles-Glendale-Long Beach, Anaheim-Santa Ana-Irvine, Riverside-San Bernardino-Ontario, San Diego-Carlsbad. The Manufacturing sector experiences the sharpest declines in SESs that are most vulnerable to cascading unemployment (*D*-*F*).

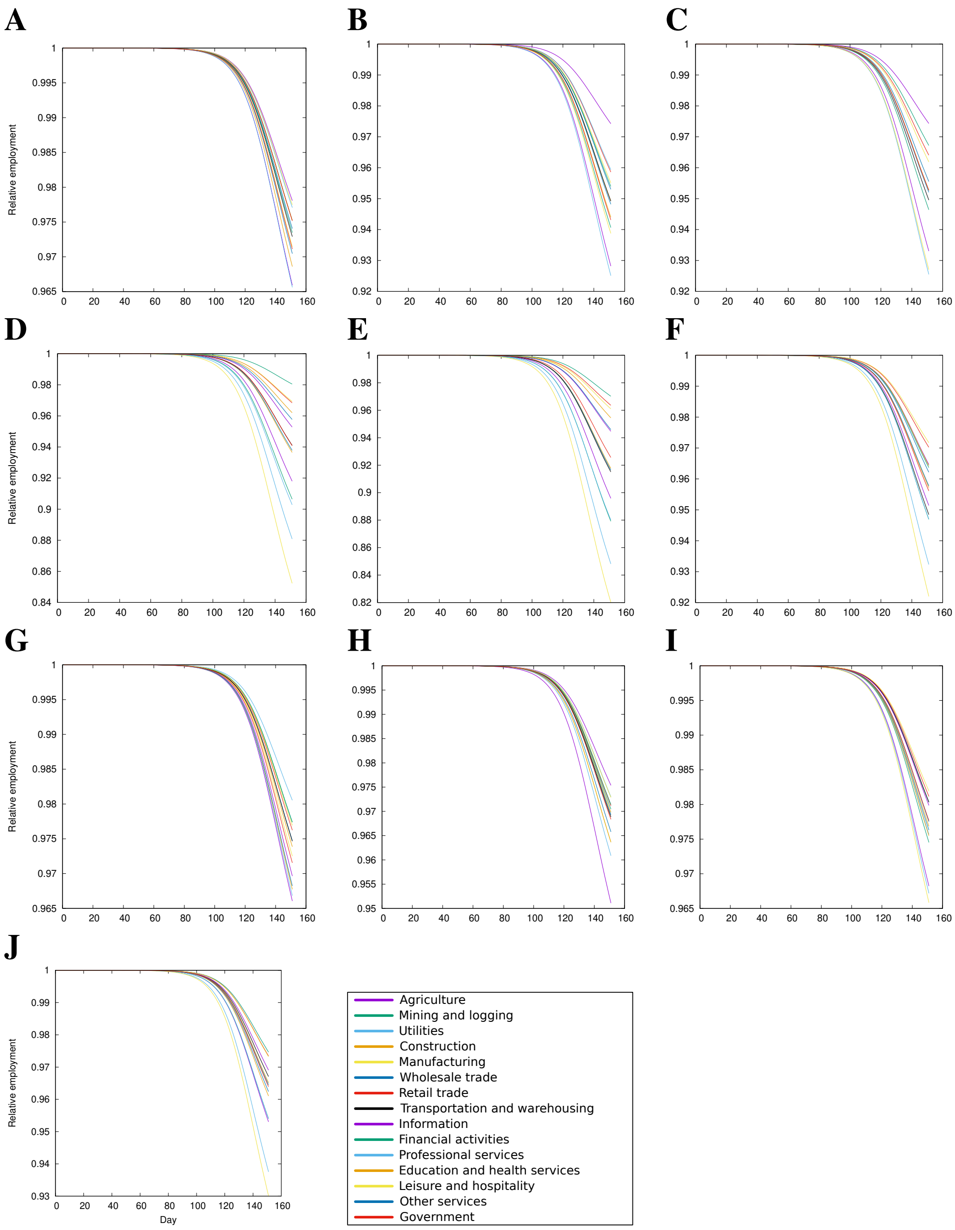

Figure S2. Relative employment decline per sector per SES. (*A*)-(*J*) respectively: Oakland-Berkeley-Livermore, San Francisco-San Mateo-Redwood City, San Jose-Sunnyvale-Santa Clara, Stockton-Lodi, Fresno, Oxnard-Thousand Oaks-Ventura, Los Angeles-Glendale-Long Beach, Anaheim-Santa Ana-Irvine, Riverside-San Bernardino-Ontario, San Diego-Carlsbad. The Manufacturing sector experiences the sharpest declines in SESs that are most vulnerable to cascading unemployment (*D*-*F*).

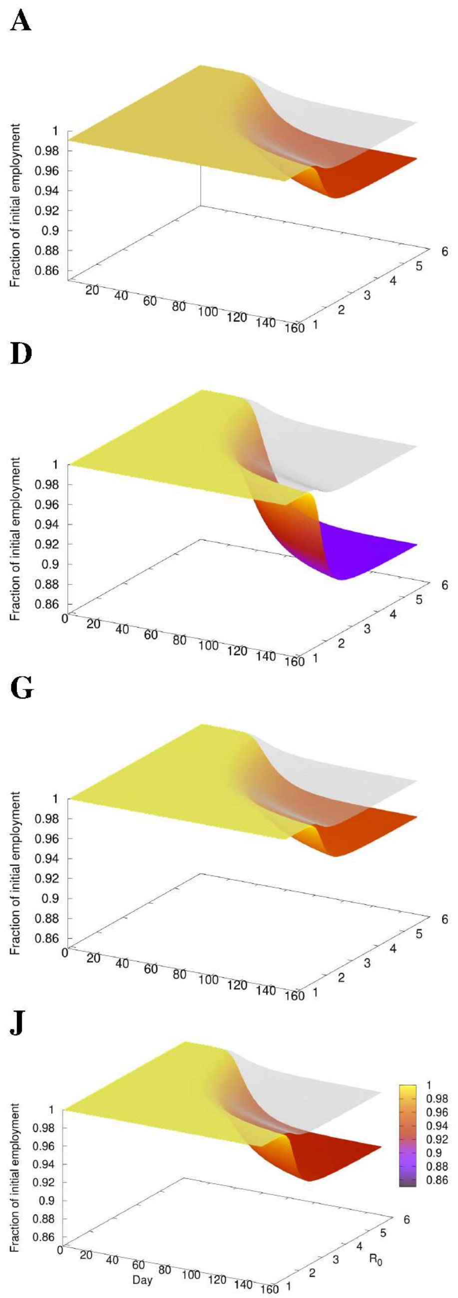

Figure S3. Total dynamics of all sectors for each SES over a R_0 range of 0.9-6.0. Upper grey surface is disease-caused losses, and lower surface shows the resulting economic cascades. Color spectrum is the fraction of initial total employment (February, 2020). See S1 Fig for key to plots.

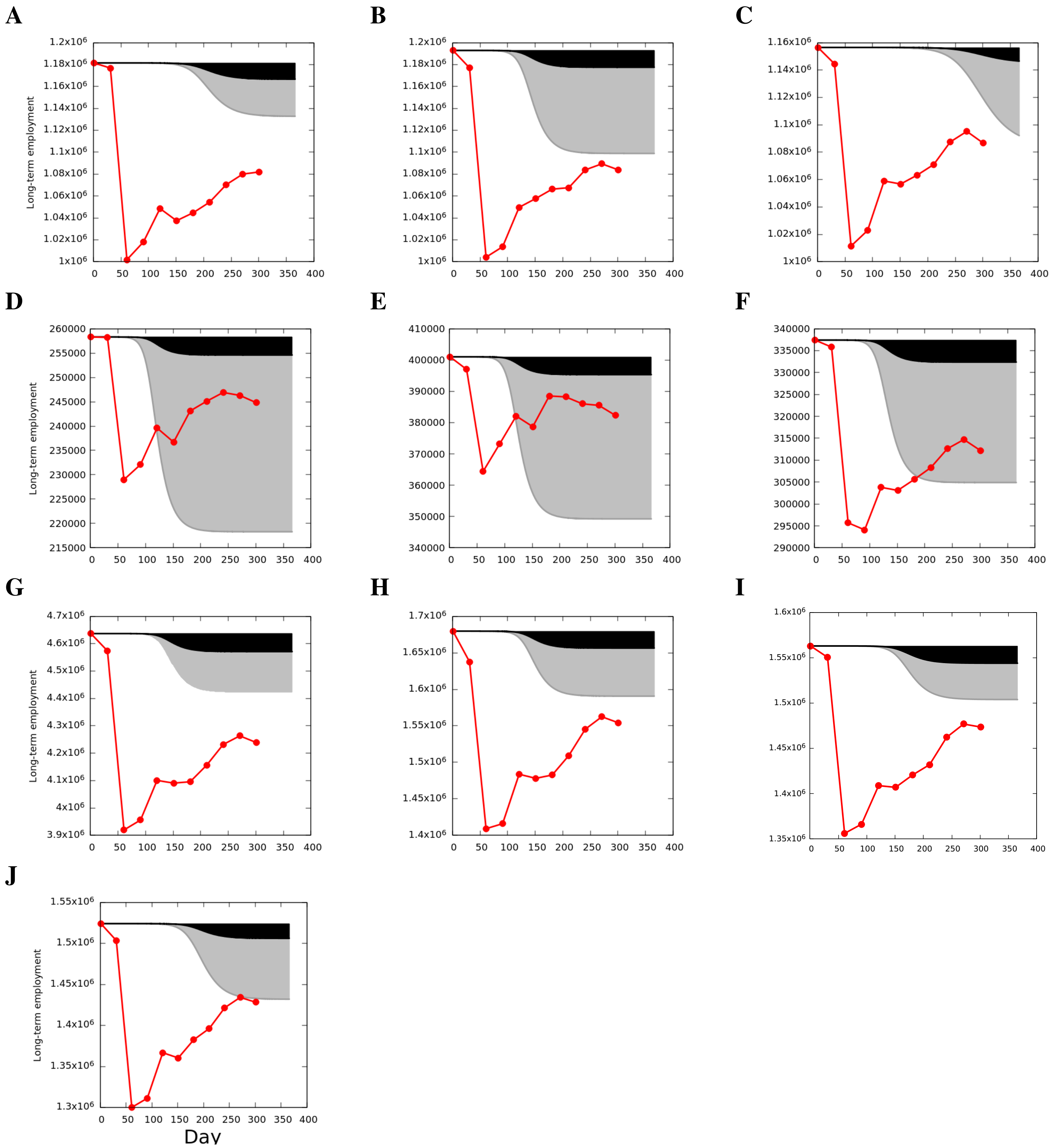

Figure S4. Comparisons of unemployment forecast by the business-as-usual model and actual unemployment of March to August, 2020. See text Fig 7 for an explanation of the plots. Key to SES plots as given in S1 Fig.